Materials Science and Engineering A 554 (2012) 116–121

Contents lists available at SciVerse ScienceDirect

Materials Science and Engineering A

journal homepage: www.elsevier.com/locate/msea

Enhanced mechanical properties of columnar grained-nanotwinned Cu films on compliant substrate via multilayer scheme

J.Y. Zhang [a], P. Zhang [a], R.H. Wang [b], G. Liu [a,*], G.J. Zhang [b], J. Sun [a]

[a] State Key Laboratory for Mechanical Behavior of Materials, Xi'an Jiaotong University, Xi'an 710049, China
[b] School of Materials Science and Engineering, Xi'an University of Technology, Xi'an 710048, China

ARTICLE INFO

Article history:
Received 15 February 2012
Received in revised form 24 May 2012
Accepted 8 June 2012
Available online 15 June 2012

Keywords:
Twins
Thin films
Nanostructured multilayers
Ductility

ABSTRACT

The columnar-grained nanotwinned (cg-nt) Cu films exhibit high strength but low ductility. By introducing the nanocrystalline Cr layers into cg-nt-Cu films forming Cu/Cr nanostructured multilayers, it is found that the number of twins per grain in Cu as well as the twins density decreases with reducing Cu layer thickness, which are analyzed by "growth accident" related twins formation models. The suppression of twin formation via multilayer scheme significantly enhanced the ductility of cg-nt-Cu films without sacrificing their strength.

1. Introduction

Structural applications of nanostructured metallic materials often require both high strength and good ductility. Strengthening materials traditionally involves the controlled creation of internal defects and boundaries so as to obstruct dislocation motion. Such strategies invariably compromise ductility. Recently, numerous attempts have been made to enhance ductility of nanostructured materials [1–5], among which introduction of nano-scale twins is an effective way to achieve coexisting high strength and high ductility by tailoring the twins thickness at room temperature [4,6]. Unlike to the random oriented-nanotwinned (nt) Cu foils [4], Zhang et al. [5] found that although the epitaxial columnar-grained nanotwinned (cg-nt) Cu foils with thickness ~20 μm exhibited high hardness/strength (~3.5/1.2 GPa) but quite low ductility (~1–2%). The high strength can be attributed to the thickness of individual twins and spacing between twins and the alignment of twin boundaries parallel to the tensile axis, while the low ductility is mainly caused by the columnar microstructure in film thickness direction favorable for the propagation of microcrack along the grain boundaries. It is generally accepted that when a freestanding thin films plastically deformable metal film is stretched, it ruptures by strain localization, and the elongation is less than a few percent [7–9]. When the thin film is deposited on a polymer substrate, however, strain localization can be retarded by the substrate [10,11], exhibiting high tensile ductility [12–14]. In parallel, Wang et al. [3] recently proposed a valuable scheme to significantly enhance the plasticity of (nano)crystalline materials by introducing amorphous layers forming nanolaminates to achieve good strain compatibility (elongation to failure ~13.8%). Moreover, Zhang et al. [15] found maxima ductility and fracture toughness in both nanostructured Cu/Nb and Cu/Zr multilayers at a critical layer thickness, due to the constraining effect of ductile Cu layer on brittle Nb and Zr layer. Therefore, it is worthy to question that (i) whether the mechanical properties of cg-nt-Cu films on compliant substrate can be improved by multilayer scheme, and (ii) how the microstructure feature of cg-nt-Cu films (e.g., twins density, twins thickness and twins spacing) effected by the heterogeneous interfaces.

In this paper, the Cu/Cr NMFs deposited on compliant polyimide substrates are chosen as the model materials (this configuration is similar to that of flexible electronics and benefits to suppress strain localization [10,13,14]). We reported that the significantly improved ductility of cg-nt-Cu films deposited on polyimide substrate by through embedding nanocrystalline Cr layer into them to form nanostructured metallic multilayer films (NMFs) and the layer thickness dependent twins density of Cu.

2. Experimental procedure

Two series of 500-nm-thick Cu/Cr NMFs were deposited on polyimide (Kapton) substrate by means of direct current (DC) magnetron sputtering at room temperature. The chamber was evacuated to a base pressure of $\sim 7 \times 10^{-8}$ Torr prior to sputtering, and $1.0–3.0 \times 10^{-3}$ Torr Ar were used during deposition. The

* Corresponding author.
E-mail address: lgsammer@mail.xjtu.edu.cn (G. Liu).

0921-5093/$ – see front matter © 2012 Elsevier B.V. All rights reserved.
http://dx.doi.org/10.1016/j.msea.2012.06.023

deposition rates were 0.6 and 0.55 nm/s for Cu and Cr, respectively. The first ones have equal individual layer thickness, i.e., modulation ratio $\eta = 1$ (η defined the ratio of Cr layer thickness h_{Cr} to Cu layer thickness h_{Cu}, $\eta = h_{Cr}/h_{Cu}$) and a wide range of layer thickness spanning from 10 to 250 nm. The second ones have equal modulation period λ ($\lambda = h_{Cr} + h_{Cu} = 25$ nm and 50 nm, respectively) with η spanning from 0.11 to 2.0. In film deposition, the first layer on the polyimide substrate was Cr and the cap layer was Cu. The as-deposited Cu/Cr NMFs were annealed at 150 °C for 2 h to stabilize the microstructure and eliminate the residual stress. The X-ray diffraction (XRD) experiment was carried out using an improved Rigaku D/max-RB X-ray diffractometer with Cu Kα radiation and a graphite monochromator to determine the crystallographic texture and the residual stress by using "$\sin^2\psi$ method" [16–18]. Transmission electron microscopy (TEM) observation was performed using a JEOL-2100F high-resolution transmission electron microscope (HRTEM) with an acceleration tension of 200 kV to observe the modulation structure and the interface structure and the growth twins. The number of grains containing twins per 100-grains (N_G) was determined from numerous TEM images about ~1000 grains included, as well as the number of twins per grain (N_T) at $h_{Cu} > 10$ nm to simply estimate the twins density (P, proportional to the number of twins boundaries intersected by a straight line of unit length for the statistical results). For comparison reasons, single-layer monolithic cg-nt-Cu and Cr films with thicknesses (h) in the 50–500 nm range were also synthesized on the dog-bone shaped polyimide substrate by same deposition conditions and followed the same treatment as mentioned above.

Uniaxial tensile testing was carried out by using a Micro-Force Test System (MTS® Tytron 250) at a constant strain rate of $1 \times 10^{-4}\ s^{-1}$. Dog-bone shaped samples for testing had a total length of 65 mm, and a gauge section of 30 mm in length and 4 mm in width. During tensile testing, the force and displacement were automatically recorded by machine and a high-resolution laser detecting system, respectively, which can be subsequently conversed into stress–strain curve of the films by subtracting the load–displacement data of the pure substrate from the total ones of the systems [15,19], as shown in Fig. 1. The critical macroscopic strain (ε_C, measured in situ using an electrical resistance change method (ERCM) [15–17,19] during the tensile test) characterizing of microcrack formation at microscopic level, rather than rupture strain or elongation, is used to represent the deformability or ductility for all the conductive multilayers. The rationale behind this method is that the electrical resistance of metallic film is very sensitive to the presence of the microcracks, which may well be undetectable under the microscope.

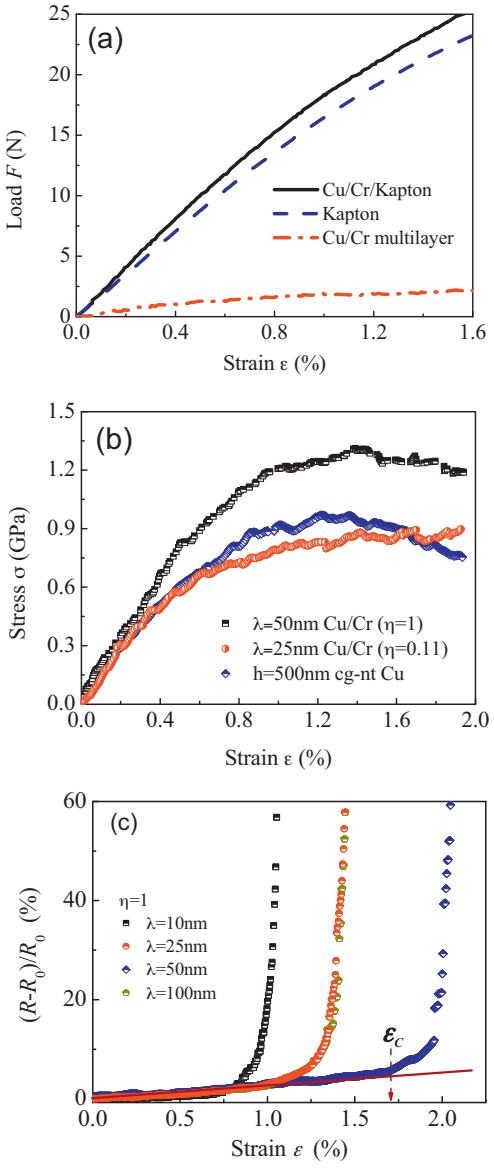

Fig. 1. (a) The force–strain curve of Cu/Cr multilayers with $\lambda = 50$ nm obtained by subtracting the load–displacement data of the Kapton substrate from the Cu/Cr/Kapton systems. (b) The stress–strain curves of Cu/Cr multilayers and cg-nt Cu films. (c) The dependence of electrical resistance change $\Delta R/R_0 = (R - R_0)/R_0$ on strain ε for Cu/Cr multilayers with $\lambda = 10$, 25, 50 and 100 nm, where R_0 is the initial resistance (at strain $\varepsilon = 0$) of the multilayers and R is the resistance of the multilayers at strain ε. The critical strain ε_C is defined as the curve deviated from the linear stage.

3. Results and discussion

3.1. Microstructure

X-ray diffraction (XRD) patterns of Cu/Cr NMFs revealed a strong ⟨1 1 1⟩ out-of-plane texture for the Cu layers and a weak ⟨1 1 0⟩ out-of-plane texture for Cr layers, while the in-plane orientations are random. By using XRD and the "$\sin^2\psi$ method", the residual tensile stresses were determined about 200 ± 100 MPa for all the annealed Cu/Cr NMFs with different λ and η, which is far lower than their yield strength [16–18].

Typical cross-sectional views of some Cu/Cr NMFs from the transmission electron microscopy (TEM) observations are displayed in Fig. 2, showing clear modulation structure and columnar grains in the Cu layers and ultra-fine nanocrystals in the Cr layers. The in-plane grain size of Cu is almost independent of layer thickness. HRTEM observations shown in Fig. 2(d) and (f) indicate insignificant intermixing at the interface between Cu and Cr. As can be seen from Fig. 2, there are growth twins in the Cu/Cr NMFs.

It is revealed that the residual stresses for the cg-nt Cu and Cr films are in range of 200 ± 50 and 200 ± 100 MPa, respectively, and independent of h. Some representative TEM images are displayed in Fig. 3, from which one can see that the high density twins (average twins spacing is $\sim 8 \pm 3$ nm) in Cu and nanocrystalline Cr single layer films without columnar porosity.

3.2. Formation of growth twins

With regard to the formation of growth twins, Jiang et al. [20] have pointed out that they can be formed by growth encounter and growth accident mechanisms, which are analogous to the models described for twins obtained in solid-state reactions (e.g., recrystallization) and solidification involving fcc metals [21]. Briefly, in

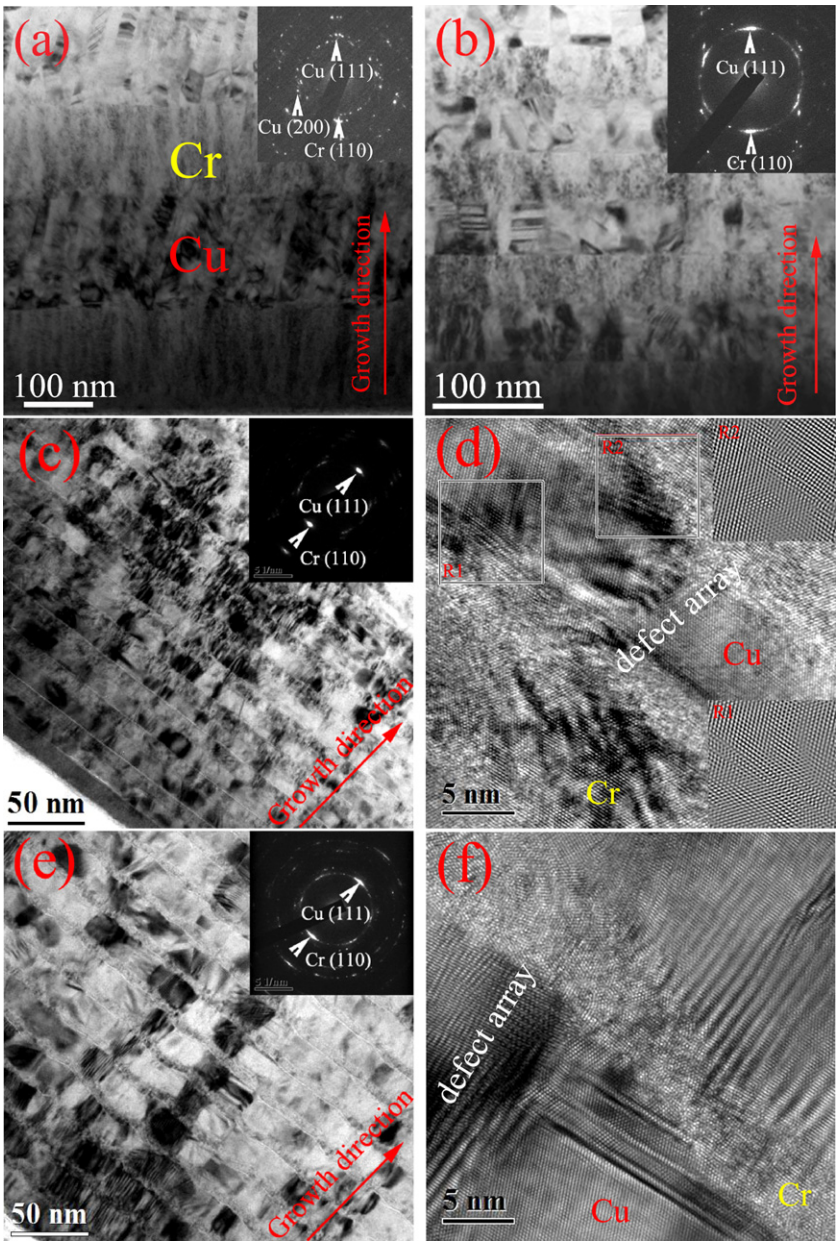

Fig. 2. Bright-field cross-sectional TEM micrographs showing typical microstructure of the Cu/Cr NMFs with $\eta = 1.0$ ((a) $\lambda = 250$ nm, (b) $\lambda = 100$ nm and (c) $\lambda = 25$ nm) and (e) $\eta = 0.33$ ($\lambda = 25$ nm). Insert is the corresponding selected area diffraction patterns (SADP). (d) and (f) showing the interface structure and twins in Cu/Cr NMFs with $\lambda = 25$ nm ((d): $\eta = 1.0$ and (f) $\eta = 0.33$). Insets in (d) show the inverse fast Fourier transform of Region 1 (R1) and Region 2 (R2), respectively.

the growth accident model [22–24], it is suggested that a coherent twin boundary forms at a migrating grain boundary due to the stacking sequence of the {1 1 1} atomic planes lost by accident during perpendicular growth under energetically favorable conditions. In a grain encounter model [25], different grains initially separated "encounter" each other during grain growth. A perpendicular twin boundary will form when these crystallites with different orientations come together [20]. Depending on the habit plane, the boundary is usually incoherent or semicoherent [26] with a relatively large energy. If these grains happen to be in twin orientation to each other, the boundary between them becomes a coherent twin boundary by reorienting itself [21]. In our case, the formation of twins can also be ascribed to the "growth accident" during the unequilibrium deposition process [20,27,28].

On the other hand, the average twins spacing ($\sim 8 \pm 3$ nm) in the Cu layer may be interpreted in terms of a thermodynamic model developed for the formation of growth twins in sputter-deposited austenitic stainless steel thin films [29]. The model predicts that during vapor deposition twinned nuclei will form at rates comparable to defect-free nuclei if the free energy change from vapor to solid is comparable for the perfect and twinned nuclei. This happens when (i) the deposited material has low stacking fault and twin boundary energies, and (ii) the deposition rate is high. For Cu with a relatively low stacking fault energy of approximately 45 mJ/m^2, growth faults and twins are predicted to form at deposition rates of a nanometer/second or higher at room temperature.

3.3. Layer thickness dependent twin density

Based on the TEM images, the statistical results of the h_{Cu} dependent N_G and N_T are respectively shown in Fig. 4(a) and (b), from which one can see that, as h_{Cu} is reduced, N_G and N_T decreased as

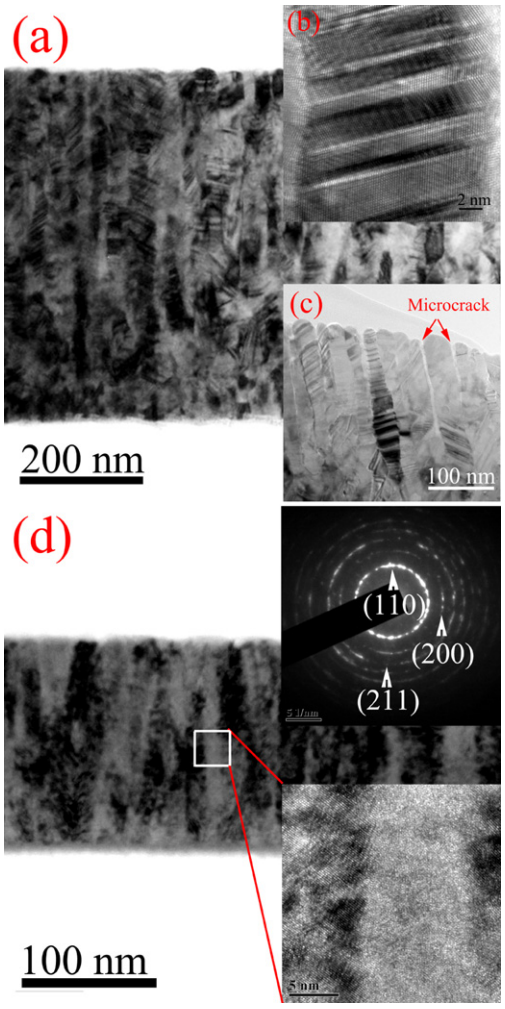

Fig. 3. Bright-field cross-sectional TEM micrographs showing typical microstructure of (a) the 500-nm-thick cg-nt-Cu, (b) the twins, (c) the tensile tested 275-nm-thick cg-nt-Cu films and (d) the 150-nm-thick Cr films. Insets in (d) are the magnification of boxed area and the corresponding selected area diffraction patterns (SADP), respectively.

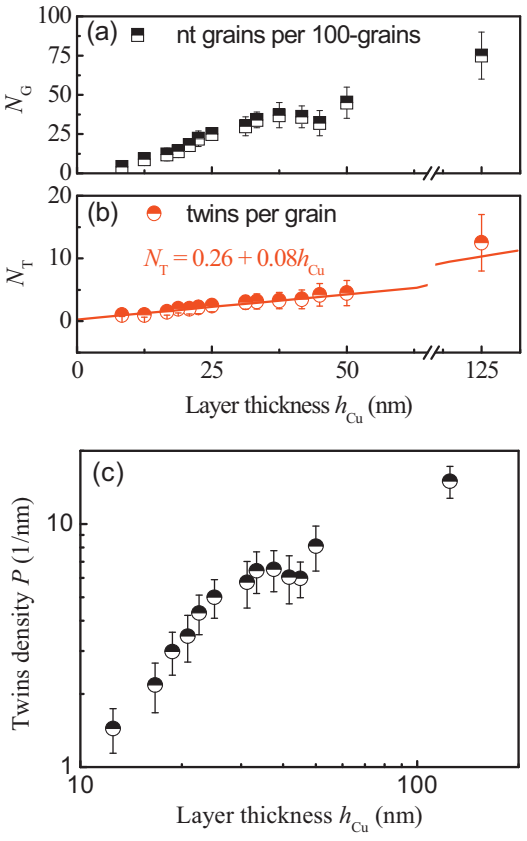

Fig. 4. The statistical results of (a) the number of twinned grain per 100-grains (N_G), (b) the number of twins grain per grain (N_T) and (c) the twins density (P) of NMFs as a function of Cu layer thickness.

well. The most striking feature in Fig. 4(b) is that the formation of twins in the grains is governed by a "linear law of formation" [30], which can be expressed by a simple equation

$$N_T = A + K_T h_{Cu} = 0.26 + 0.08 h_{Cu}. \quad (1)$$

where A is a constant and K_T is the slope reflecting the rate of twin formation related to layer thickness. The linear dependence of N_T on h_{Cu} found in the present work, can also be explained on the basis of the "growth accident". During h_{Cu} increase (i.e., grain growth) the average migration distance increases with the final grain size achieved and N_T increases proportionally to h_{Cu}. Accordingly, if h_{Cu} increased linearly during grain growth, so should N_T increases. It is reasonable for that the deposition rate of Cu is same for all the NMFs and h_{Cu} is solely determined by the deposition time and is also supported by the average twins spacing is same ($\sim 8 \pm 3$ nm) at different h_{Cu} of Cu/Cr NMFs. The density of twins P thus can be simply expressed as

$$P \approx 2N_G \frac{N_T}{h_{Cu}}. \quad (2)$$

From Fig. 4(c) one can see that the P decreases with reducing h_{Cu}, which indicates that the smaller length scale is, the less twin is. The decrease in density of twins in Cu layer suggests that the twinning process can be suppressed by introduction of heterogeneous interface, which tailors the microstructure and mechanical properties of the materials.

3.4. Heterogeneous interfaces effects on mechanical properties

First, we reveal the number of heterogeneous interfaces effects on the mechanical properties by introducing Cr layer with different layer thickness into nt-Cu films. Fig. 5(a) shows the dependence of ε_C of Cu/Cr NMFs with constant $\eta = 1$ on h_{Cu} or h. Both the single-layer nt-Cu and Cr films exhibited a monotonic decrease of ε_C as h is reduced, and their ductility quite closes to each other. Compared with Niu et al.'s [19] result, the nt-Cu film behaves the same way as that of poly-Cu films but shows far lower ε_C. The low ductility of nt-Cu films is ascribed to the columnar grains and the weak grain boundaries, which are difficult to block the microcrack propagate. Indeed, in Fig. 3(c), some microcracks are observed at grain boundaries. Interestingly, in Fig. 5(a) one can see that over this h_{Cu} range the ε_C of Cu/Cr NMFs increases first, followed by a peak at a critical $h_{Cu}^{cri} \sim 25$ nm (or $\lambda^{cri} \sim 50$ nm). Below h_{Cu}^{cri}, ε_C decreases with reducing h_{Cu}, similar to the behavior of single-layer films, while above h_{Cu}^{cri}, a smaller h_{Cu} leads to higher ε_C. The unusual length scale dependent ductility observed here can be reasonably explained by considering the competing thickness effects on the size of the microcracks initiated in the Cr layers and on the role of the ductile Cu layer in blocking crack propagation, as illustrated in our previous paper [15–17]. The peak ε_C of the $\lambda = 50$ nm Cu/Cr NMFs with yield strength ~1280 MPa is a factor of 2 higher than that of $h = 500$ nm monolithic cg-nt-Cu films with yield strength ~820 MPa. This indicates that the mechanical properties of cg-nt-Cu films can be improved sharply by tailoring the number of

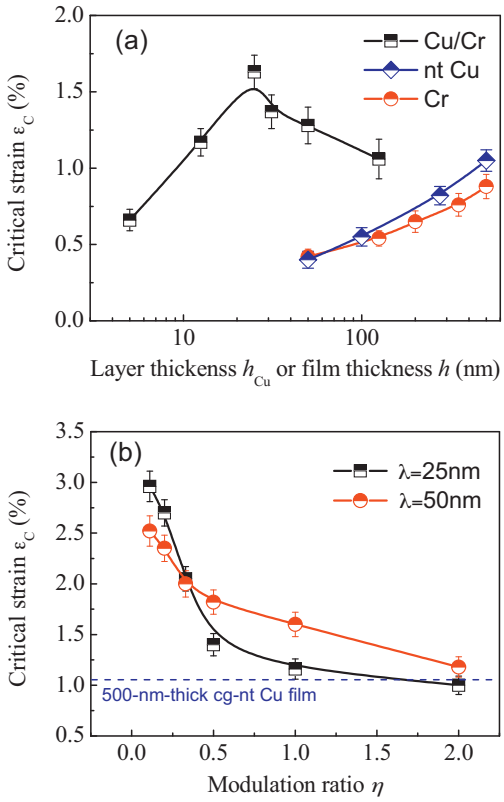

Fig. 5. Dependence of ε_C on (a) h_{Cu} for the $\eta = 1$ Cu/Cr NMFs and on h for the single-layer Cr and nt-Cu films, and on (b) η for the constant λ-Cu/Cr NMFs, respectively. The ε_C of 500-nm-thick nt-Cu films is shown in (b), see the horizontal dash line.

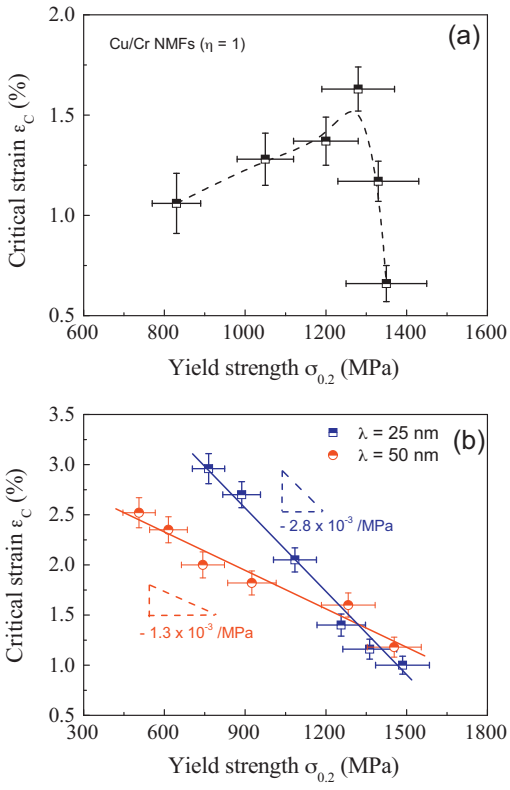

Fig. 6. (a) Relationship between ε_C and $\sigma_{0.2}$ in the Cu/Cr NMFs with $\eta = 1$. (b) Scaling relationship between ε_C and $\sigma_{0.2}$ in the Cu/Cr NMFs with $\lambda = 25$ and 50 nm. The data of strengths are from Refs. [17,18].

heterogeneous interfaces, which can stop the propagation of micro-cracks.

Next, we focus on effect of heterogeneous Cr layer thickness on the ductility at a given number of heterogeneous interfaces. For the Cu/Cr NMFs with constant λ, ε_C monotonically decreases with increasing η, see the experimental results in Fig. 5(b). The striking feature is that, at a given η, as η reduces down to below a critical η^{cri} (~0.33), the ductility of Cu/Cr NMFs with small $\lambda = 25$ nm is higher than that of Cu/Cr NMFs with $\lambda = 50$ nm. While, above η^{cri}, larger λ, higher ε_C (ductility) at a given η. This means that the Cu/Cr NMFs with small η (below η^{cri}) and λ can exhibit high ductility and high strength, which is significant for engineering applications. This can still be elucidated by considering the fracture mechanism in the NMFs composed of alternating soft/hard layers [15–17]. One can also see that the Cu/Cr NMFs with constant λ exhibited higher ductility (ε_C) than that of nt-Cu films, and that the ductility of $\lambda = 25$ nm ones with yield strength ~784 MPa at $\eta = 0.11$ is factor of 3 greater than that of 500 nm-thick cg-nt-Cu films with yield strength ~820 MPa. It suggests that the deformability of cg-nt-Cu films can be enhanced remarkable without losing their strength.

3.5. The relationship between strength and ductility

Generally, the strength and tensile ductility of materials are exclusive to each other, i.e., the higher strength, the lower tensile ductility. This is consistent with the results observed in the Cu/Cr NMFs with constant λ (see Fig. 6(b)). Interestingly, in this regard, there is a linear scaling law between the strength and ductility, as is explained in our previous work in detail [17]. In contrast, for the Cu/Cr NMFs with constant η, both the strength and ductility increase simultaneously as reducing λ from 250 down to the critical $\lambda^{cri} \sim 50$ nm, while below which the ductility sharply decrease with increasing strength (see Fig. 6(a)). It is suggested that it is possible to artificially control the constituent phases or geometrical configures in NMFs to achieve best combination of strength and ductility.

4. Conclusions

The present results reveal that the columnar-grained nt-Cu films on compliant substrate can be toughened by multilayer scheme and that optimized mechanical properties can be achieved at a critical length scale ~50 nm. The introduction of heterogeneous interface can significantly suppress twin formation. The number of twins per grain increases linearly with increasing Cu layer thickness, following the "linear law of formation".

Acknowledgements

This work was supported by the 973 Program of China (Grant No. 2010CB631003), the 111 Project of China (B06025) and the National Natural Science Foundation of China (50971097). GL thanks the support of Fundamental Research Funds for the Central Universities, GJZ thanks the support of the Program for New Century Excellent Talents in University (Grant No. NCET-10-0876) and JYZ thanks the financial support of China Scholarship Council (CSC).

References

[1] E. Ma, JOM 58 (2006) 49.
[2] Y. Wang, M. Chen, F. Zhou, E. Ma, Nature 419 (2002) 912.
[3] Y.M. Wang, J. Li, A.V. Hamza, J.T.W. Barbee, Proc. Natl. Acad. Sci. U. S. A. 104 (2007) 11155.

[4] L. Lu, X. Chen, X. Huang, K. Lu, Science 323 (2009) 607.
[5] X. Zhang, H. Wang, X.H. Chen, L. Lu, K. Lu, R.G. Hoagland, A. Misra, Appl. Phys. Lett. 88 (2006) 173116.
[6] Y.F. Shen, L. Lu, Q.H. Lu, Z.H. Jin, K. Lu, Scr. Mater. 52 (2005) 989.
[7] H. Huang, F. Spaepen, Acta Mater. 48 (2000) 3261.
[8] R.D. Emery, G.L. Povirk, Acta Mater. 51 (2003) 2067.
[9] R.D. Emery, G.L. Povirk, Acta Mater. 51 (2003) 2079.
[10] T. Li, Z. Suo, Int. J. Solids Struct. 43 (2006) 2351.
[11] T. Li, Z. Suo, Int. J. Solids Struct. 44 (2007) 1696.
[12] Y. Xiang, T. Li, Z. Suo, J.J. Vlassak, Appl. Phys. Lett. 87 (2005) 161910.
[13] N. Lu, X. Wang, Z. Suo, J. Vlassak, Appl. Phys. Lett. 91 (2007) 221909.
[14] N. Lu, Z. Suo, J.J. Vlassak, Acta Mater. 58 (2010) 1679.
[15] J.Y. Zhang, X. Zhang, R.H. Wang, S.Y. Lei, P. Zhang, J.J. Niu, G. Liu, G.J. Zhang, J. Sun, Acta Mater. 59 (2011) 7368.
[16] J.Y. Zhang, G. Liu, X. Zhang, G.J. Zhang, J. Sun, E. Ma, Scr. Mater. 62 (2010) 333.
[17] J.Y. Zhang, X. Zhang, G. Liu, G.J. Zhang, J. Sun, Scr. Mater. 63 (2010) 101.
[18] J.Y. Zhang, X. Zhang, G. Liu, G.J. Zhang, J. Sun, Mater. Sci. Eng. A 528 (2011) 2982.
[19] R.M. Niu, G. Liu, C. Wang, G. Zhang, X.D. Ding, J. Sun, Appl. Phys. Lett. 90 (2007) 161907.
[20] H. Jiang, T.J. Klemmer, J.A. Barnard, W.D. Doyle, E.A. Payzant, Thin Solid Films 315 (1998) 13.
[21] C.S. Pande, M.A. Imam, B.B. Rath, Metall. Mater. Trans. A 21 (1990) 2891.
[22] H. Gleiter, Acta Metall. 17 (1969) 1421.
[23] R.L. Fullman, J.C. Fisher, J. Appl. Phys. 22 (1951) 1350.
[24] S. Mahajan, C.S. Pande, M.A. Imam, B.B. Rath, Acta Mater. 45 (1997) 2633.
[25] J.P. Nielsen, Acta Metall. 15 (1967) 1083.
[26] D.G. Brandon, Acta Metall. 14 (1966) 1479.
[27] A.H. King, Phys. Status Solidi (a) 76 (1983) 629.
[28] K. Meinel, M. Klaua, H. Bethge, Phys. Status Solidi (a) 110 (1988) 189.
[29] X. Zhang, A. Misra, H. Wang, T.D. Shen, M. Nastasi, T.E. Mitchell, J.P. Hirth, R.G. Hoagland, J.D. Embury, Acta Mater. 52 (2004) 995.
[30] R.A. Varin, J. Kruszynska, Acta Metall. 35 (1987) 1767.